Single-Molecule Measurements of the Binding between Small Molecules and DNA Aptamers

ARTICLE *in* ANALYTICAL CHEMISTRY · JUNE 2012

Impact Factor: 5.64 · DOI: 10.1021/ac300427d · Source: PubMed

6 AUTHORS, INCLUDING:

Zhongbo Yu
Delft University of Technology
20 PUBLICATIONS **351** CITATIONS
SEE PROFILE

Deepak Koirala
University of Chicago
25 PUBLICATIONS **337** CITATIONS
SEE PROFILE

Simon M Mwongela
Georgia Gwinnett College
12 PUBLICATIONS **283** CITATIONS
SEE PROFILE

Hanbin Mao
Kent State University
52 PUBLICATIONS **1,744** CITATIONS
SEE PROFILE

analytical chemistry

Article

pubs.acs.org/ac

Single-Molecule Measurements of the Binding between Small Molecules and DNA Aptamers

Philip M. Yangyuoru,[‡] Soma Dhakal,[‡] Zhongbo Yu,[‡] Deepak Koirala,[‡] Simon M. Mwongela,[†] and Hanbin Mao*[,‡]

[†]School of Science & Technology, Georgia Gwinnett College, Lawrenceville, Georgia 30043, United States

[‡]Department of Chemistry and Biochemistry, Kent State University, Kent, Ohio 44242, United States

Supporting Information

ABSTRACT: Aptamers that bind small molecules can serve as basic biosensing platforms. Evaluation of the binding constant between an aptamer and a small molecule helps to determine the effectiveness of the aptamer-based sensors. Binding constants are often measured by a series of experiments with varying ligand or aptamer concentrations. Such experiments are time-consuming, material nonprudent, and prone to low reproducibility. Here, we use laser tweezers to determine the dissociation constant for aptamer–ligand interactions at the single-molecule level from only one ligand concentration. Using an adenosine 5′-triphosphate disodium salt (ATP) binding aptamer as an example, we have observed that the mechanical stabilities of aptamers bound with ATP are higher than those without a ligand. Comparison of the change in free energy of unfolding (ΔG_{unfold}) between these two aptamers yields a ΔG of 33 ± 4 kJ/mol for the binding. By applying a Hess-like cycle at room temperature, we obtained a dissociation constant (K_d) of 2.0 ± 0.2 μM, a value consistent with the K_d obtained from our equilibrated capillary electrophoresis (CE) (2.4 ± 0.4 μM) and close to that determined by affinity chromatography in the literature (6 ± 3 μM). We anticipate that our laser tweezers and CE methodologies may be used to more conveniently evaluate the binding between receptors and ligands and also serve as analytical tools for force-based biosensing.

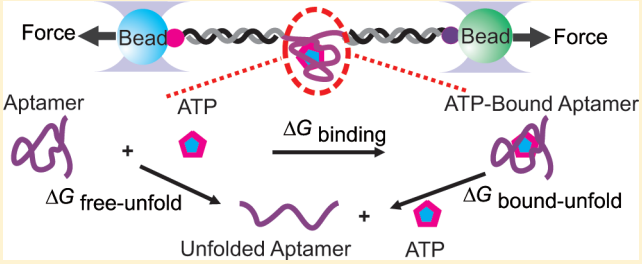

The interaction between nucleic acids and small molecules is continuously generating significant interest due to their widespread use in analytical and bioanalytical applications. Specific nucleic acids such as aptamers have been shown to bind not only to nucleic acids but also to non nucleic acid targets such as small molecules,[1,2] proteins,[3] and cells.[4] Aptamers are single-stranded ligand-binding nucleic acids with affinity and selectivity comparable to those of antibodies.[5,6] Compared to antibodies, DNA aptamers are easier to obtain, more stable, and more resistant to biodegradation. As such, they are suitable for demanding conditions such as extreme pH and temperatures. These properties render them ideal candidates for sensors used in medical diagnostics and environmental monitoring.[7]

The binding affinity between an aptamer and a ligand is a critical factor to reflect the sensitivity of aptamer-based biosensors.[8] Conventionally, the binding is measured by techniques such as electrochemical detection,[9,10] fluorescence,[11] colorimetric[12] or surface plasma resonance (SPR) based detection,[13] and capillary electrophoresis (CE) separation,[14−16] among others.[17] At the single-molecular level, atomic force microscopy (AFM) has been recently used to determine the adenosine 5′-triphosphate disodium salt (ATP) binding to an aptamer made of two independently split DNA strands.[18] Single-molecule fluorescence resonance energy transfer (FRET) has also been explored to evaluate the binding of a DNA aptamer with its binding target, vascular endothelial growth factor (VEGF).[19]

However, a majority of these methods require a series of experiments with varying ligand or aptamer concentrations to determine the dissociation constant. Apart from being tedious and time-consuming, such experiments are prone to a decreased signal-to-noise ratio due to run-to-run variations. Another disadvantage is that they require a substantial amount of materials. This becomes problematic especially in drug screening processes where the amount of a sample is often limited. As an alternative, here, we employ a laser tweezers instrument to determine the dissociation constant between ATP and a DNA aptamer by using only one concentration of ATP.

Developed in the 1980s,[20] laser tweezers have been used extensively to probe the mechanical stabilities not only for DNA[21,22] and RNA[23−26] but also for proteins[27] at the single-molecule level. Recently, we have extended this method to investigate the interaction between a DNA G-quadruplex and its ligand,[28] as well as to serve as a force-based biosensing platform.[29] Here, we use this technique to scrutinize the interaction between aptamers and ligands. The binding of ATP

Received: February 13, 2012
Accepted: May 22, 2012
Published: May 23, 2012

to the aptamer is expected to increase the mechanical stability of the aptamer. This increment is converted to the change in the free energy of binding ($\Delta G_{binding}$) by a Hess-like process. The $\Delta G_{binding}$ is then used to obtain the dissociation constant (K_d) of the complex, which is validated by our CE measurement. Such a force-based strategy is less prone to background noise[29] often seen in fluorescence-based methods. Our results demonstrate a strong correlation between ensemble average assays (CE) and single-molecule approaches (laser tweezers) on the binding between aptamers and small molecules.

MATERIALS AND METHODS

Materials. ATP was purchased from USB Corp., Cleveland, OH. *N*-[Tris(hydroxymethyl)methyl]glycine (Tricine) was purchased from Fisher Scientific. Trizma base (minimum 99.9% titration) was purchased from Sigma. Poly-(vinylpyrrolidone) (PVP) was obtained from Acros Organics. Nanopure water was purified by Millipore Synergy UV with a 185 nm UV lamp. The ATP aptamer and a scrambled sequence for control experiments were labeled with 6-carboxyfluorescein (FAM) to form 5′-[FAM]TAC CTG GGG GAG TAT TGC GGA GGA AGG TT-3′ and 5′-[FAM]TAG TGC GCG TGT GTG AGC AGA GTG AGA GT-3′, respectively. They were purified using HPLC by the manufacturer (Integrated DNA Technologies (IDT), Coralville, IA). Other DNA fragments were purchased from IDT and purified with polyacrylamide gel electrophoresis (PAGE).

Synthesis of the DNA Construct for Single-Molecule Studies. Preparation of the DNA construct for single-molecule mechanical unfolding studies was carried out following a previous protocol.[30] Overall, an ATP DNA aptamer fragment was sandwiched between two double-stranded DNA (dsDNA) handles (2690 and 2028 bp). The 2690 bp handle was constructed from a pEGFP plasmid (Clontech, Mountain View, CA) by *Sac*I (New England Biolabs (NEB), Ipswich, MA) and *Eag*I (NEB) digestions. It was gel purified and labeled with digoxigenin (Dig) at the 3′ end (*Sac*I end) using 18 μM Dig-dUTP (Roche, Indianapolis, IN) and terminal transferase (Fermentas, Glen Burnie, MD). To ensure complete Dig labeling, excess Dig-dUTP was used (Dig-dUTP:2690 bp DNA = 150:1). The Dig-labeled 2690 fragment was purified by ethanol precipitation. To make the 2028 bp handle, a pBR322 plasmid (NEB) was first amplified by polymerase chain reaction (PCR) using a 5′-labeled biotinylated primer, 5′-GCA TTA GGA AGC AGC CCA GTA GTA GG-3′ (IDT). The PCR product was purified by a kit (Qiagen, Germantown, MD) and digested overnight with *Xba*I restriction enzyme (NEB).

The 83-mer DNA fragment sandwiched by the 2028 and 2690 bp handles contains a single-stranded ATP aptamer sequence in the middle, 5′-ACC TGG GGG AGT ATT GCG GAG GAA GGT. This sequence is flanked by two dsDNA fragments that end with 5′-GGC CGA CGC GCT GGG CTA CGT CTT GCT GGC and 5′-CGC ATC TGT GCG GTA TTT CAC ACC GT sticking ends, to which the 2028 and 2690 bp dsDNA handles were ligated using T4 DNA ligase (NEB) and purified using a gel extraction kit (Qiagen). The final construct was ethanol precipitated, dissolved in water, and stored at −20 °C. The DNA construct with a scrambled sequence, 5′-AGT GCG CGT GTG TGA GCA GAG TGA GAG, in place of the ATP aptamer, was prepared by the same procedure.

Single-Molecule Experiments. A detailed description of the laser tweezers instrument used for the single-molecule experiment has been reported elsewhere.[31] To start the single-molecular experiment at room temperature, the appropriately diluted DNA construct prepared above (0.50 ng/μL) was incubated with anti-Dig-coated polystyrene beads (diameter 2.10 μm, Spherotech, Lake Forest, IL) for 1 h at room temperature. This allowed the DNA construct to bind to the beads through the Dig−anti-Dig linkage. The incubated sample was diluted to 800 μL in a 10 mM phosphate buffer (pH 7.4) with 100 mM KCl. Streptavidin-coated beads (diameter 0.97 μm, Bangs Laboratory) were dispersed into the same working buffer. The streptavidin-coated beads and the anti-Dig-coated beads linked with the DNA construct were injected separately into a reaction chamber through different channels. These two types of beads were captured separately by the two laser traps. The two laser-trapped beads were moved to touch against each other to allow the free end of a DNA molecule on the anti-Dig-coated bead to tether to the streptavidin-coated bead via the streptavidin−biotin linkage. The anti-Dig-coated bead, controlled by the Nano-MTA positioned in the laser tweezers instrument, was then moved away from the streptavidin-coated bead with a loading speed of ∼5.5 pN/s. A sudden drop in the tension was observed whenever there was an unfolding of a secondary structure. Single tethers were confirmed by observing the single breakage of the tether during stretching or the 65 pN plateau in force−extension ($F-X$) curves.[32] The force−extension curve for each tether was recorded in a Labview program, and data treatment was performed using programs in Matlab and Igor software. Only $F-X$ curves from single tethers were considered for data analysis. Two data points flanking the rupture event in the $F-X$ curves were used to calculate the change in contour length (ΔL) during the rupture of a folded structure according to the following equation:[22]

$$\frac{x}{L} = 1 - \frac{1}{2}\left(\frac{k_B T}{FP}\right)^{1/2} + \frac{F}{S} \quad (1)$$

where x is the end-to-end distance, L is the contour length, T is absolute temperature (298 K), F is the force, k_B is the Boltzmann constant, P = 51.95 nm[33] is the persistent length, and S = 1226 pN[33] is the elastic strength modulus.

The bias of these free energy estimations was calculated according the described method.[34] The dissipated work, 12 and 15 k_BT for unfolding at 0 and 100 μM ATP, respectively, was well within the range (∼20 k_BT) for effective bias calculations.[34]

The formation probability of a folded species is calculated by taking the ratio of $F-X$ curves that contain rupture events versus the total number of tethered $F-X$ curves.

Capillary Electrophoresis Experiments. Aliquots of ATP (0−60 μM) were added to the ATP aptamer (0.5 nM) in a 10 mM phosphate buffer (pH 7.4) with 100 mM KCl. The mixture was heated to 97 °C for 5 min followed by slow cooling to room temperature for 4 h in a Bio-Rad DNAEngine Peltier thermal cycler. Capillary electrophoresis was performed on a Beckman ProteomeLab PA800 CE system (Fullerton, CA). The machine is equipped with a laser-induced fluorescence (LIF) detector using an air-cooled 3.5 mW argon laser (Beckman Instruments), with excitation at 488 nm and emission at 520 nm, and is installed with 32 Karat 8.0 software (Beckman Instruments) for instrument control and data analysis. Separations were performed on 30 cm fused-silica capillaries (Polymicro Technologies, Phoenix, AZ) with 50 μm

dx.doi.org/10.1021/ac300427d | *Anal. Chem.* 2012, 84, 5298−5303

i.d. and 375 μm o.d. (20 cm effective length). New capillaries were preconditioned by successively flushing with 1.0 M NaOH for 30 min and rinsed with distilled deionized H_2O for 20 min at 20 psi. Samples were injected hydrodynamically at 1.0 psi for 10 s. The separation buffer was made of 25 mM Tris, 25 mM Tricine, and 0.5% PVP. During the separation the capillary column was thermostated at 25 °C, and an electric field strength of 500 V/cm was applied in the reverse polarity mode (anode at the detector).

RESULTS

Enhancement of the Mechanical Stability of an Aptamer by Small-Molecule Binding. We first investigated the mechanical stability of the ATP aptamer itself. After sandwiching the aptamer fragment between two dsDNA handles, the DNA construct was tethered between the two laser-trapped beads via biotin–streptavidin and Dig–anti-Dig antibody linkages (Figure 1A). The tension in the DNA tether

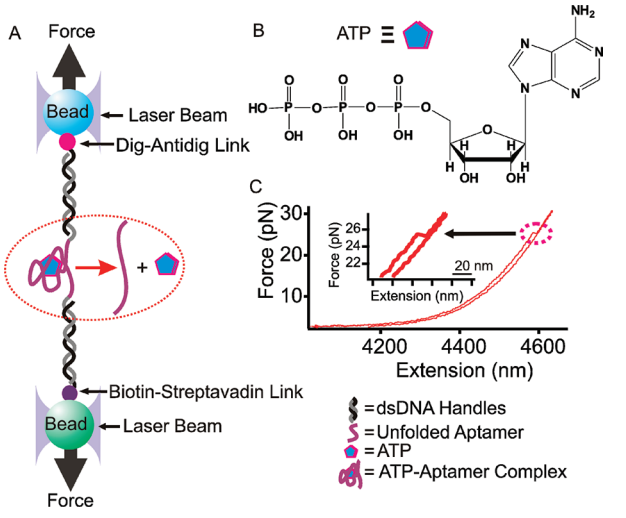

Figure 1. (A) Schematic of the experimental setup. (B) ATP structure. (C) Typical force–extension curve. The inset shows a blowup of the unfolding event denoted by the dotted circle.

was gradually increased by moving one of the trapped beads away from the other until a sudden drop in force was observed in the F–X curves (Figure 1C inset). This drop in force is associated with the unfolding of a secondary structure, most likely the aptamer, in the DNA construct. The change in contour length (ΔL; see the Materials and Methods for the calculation) was determined to be 9.2 ± 0.1 nm, a value consistent with the contour length of the 27-mer ATP aptamer.[30,35] In a control with a scramble sequence (see the Materials and Methods) that does not assume any stable conformations, no folded structure was observed (data not shown), which strongly suggests that the observed events are due to the ruptures of folded ATP aptamers. The unfolding force at which the rupture event occurred showed a most probable value of 21 pN without the ATP ligand (Figure 2A). The probability of observing these rupture events from all tethered DNA molecules is 24% (see the Materials and Methods for the calculation), suggesting a significant fraction of the aptamers is not folded.

To investigate the binding of a small molecule, the aptamer construct was incubated with 2.0 μM ATP. The rupture force histogram for this treatment revealed two populations with

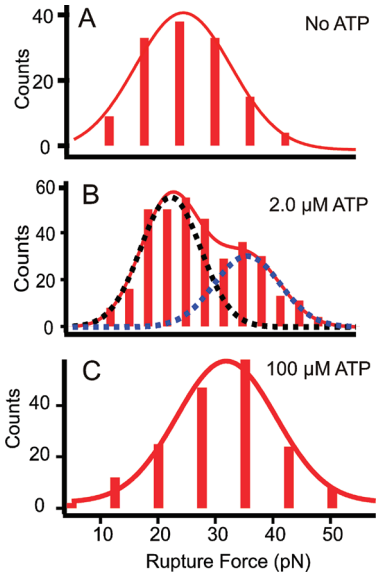

Figure 2. Unfolding force histograms of the ATP aptamer in a 10 mM phosphate buffer (pH 7.4) with ATP concentrations of (A) 0 μM, (B) 2.0 μM, and (C) 100.0 μM. Curves depict Gaussian fittings.

rupture forces centered at 21 and 38 pN (Figure 2B). On the basis of the similar rupture force, we assigned the 21 pN population as the free aptamer. After the aptamer binds to ATP, it is expected that the mechanical stability of the aptamer will increase.[28] Therefore, the 38 pN species was assigned as the ATP-bound aptamer (Figure 2B). To confirm this assignment, we increased the ATP concentration to 100 μM with the expectation that the population of the ATP-bound aptamer should increase. Indeed, this was observed in the unfolding force histogram in Figure 2C. The increase in the mechanical stability of the aptamer upon ligand binding can be exploited to further develop force-based biosensing recently developed in our laboratory.[29]

Dissociation Constant Determination at Only One Concentration of a Ligand. The dissociation constant (K_d) between the ATP and the aptamer can be calculated by the expression $\ln(K_d) = -\Delta G_{binding}/RT$, where $\Delta G_{binding}$ is the change in free energy of binding, a state function that is independent of pathways. To obtain the $\Delta G_{binding}$, we designed a Hess-like cycle[28] in which the binding of the ligand to the aptamer is rerouted to the unfolding of a free aptamer in the presence of an unbound ligand. This is followed by the formation of the ATP-bound complex from the mechanically unfolded aptamer (Figures 3 and 4). The $\Delta G_{binding}$ is then estimated from the difference in the change in free energy of unfolding (ΔG_{unfold}) for the latter two processes. Each ΔG_{unfold} is obtained using Jarzynski's equality equation[36]

$$\Delta G_{unfold} = -k_B T \ln \sum_{i-1}^{N} \frac{1}{N} \exp\left[-\frac{W_i}{k_B T}\right] \quad (2)$$

where k_B is the Boltzmann constant, T is absolute temperature, N is the number of observations, and W is the nonequilibrium work done to unfold the structure(s), which is equivalent to the hysteresis area between stretching and relaxing F–X curves (see Figure 1C as an example). Histograms for the work revealed that the average work done to unfold the free aptamer (Figure 3A) is less than that for the ATP-bound aptamer (Figure 3B), which confirms that the mechanical stability of the aptamer is

dx.doi.org/10.1021/ac300427d | Anal. Chem. 2012, 84, 5298–5303

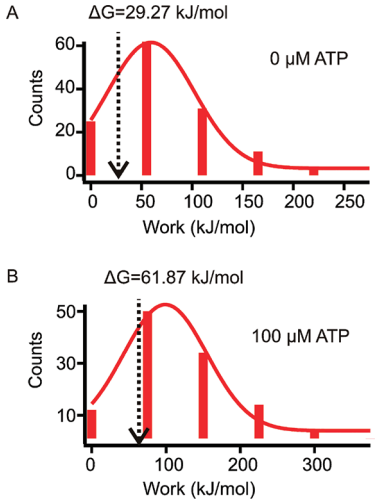

Figure 3. Histograms of the work done to unfold the free aptamer (A) and ATP-bound aptamer (B). The work is calculated at 100 μM ATP. Solid curves depict Gaussian fittings. Dotted arrows show the work equivalent to the change in free energy of unfolding (ΔG_{unfold}).

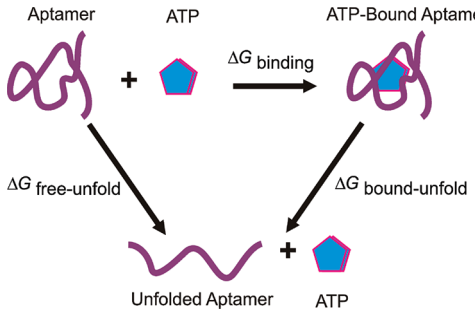

Figure 4. Hess-like cycle of the aptamer–ATP binding process used for the calculation of the $\Delta G_{binding}$ and the determination of the dissociation constant.

enhanced after ligand binding. The Jarzynski calculation yielded a $\Delta G_{free\text{-}unfold}$ of 29 ± 3 kJ/mol (bias estimation 7 kJ/mol) and a $\Delta G_{bound\text{-}unfold}$ of 62 ± 3 kJ/mol (bias estimation 8 kJ/mol). With these, $\Delta G_{binding}$ was calculated by the following expression:

$$\Delta G_{binding} = \Delta G_{free\text{-}unfold} - \Delta G_{bound\text{-}unfold} \quad (3)$$

This treatment yielded a $\Delta G_{binding}$ of −33 ± 4 kJ/mol, which led to a K_d of 2.0 ± 0.2 μM by the equation $\Delta G_{binding} = -RT \ln K_d$.

Determination of the Dissociation Constant by CE. To validate these single-molecule results, we set out to compare the K_d value with an ensemble measurement. It is known that binding affinity can be determined by capillary electrophoresis.[37,38] Therefore, the ATP aptamer was labeled with 6-carboxyfluorescein at the 5′ end and analyzed using CE-LIF.

Depicted in Figure 5 are two populations (~4.6 and ~4.2 min retention times) in the electropherogram of the 0.5 nM ATP aptamer with increasing ATP concentrations (0–60 μM). Since a significant fraction of DNA is not folded as revealed by laser tweezers experiments (see above), we ascribe the larger population (the 4.2 min peak) as unfolded aptamer and the 4.6 min population as the folded aptamer bound with or without ATP. The difference in the elution time reflects the variation in the size and charge between folded and unfolded ATP

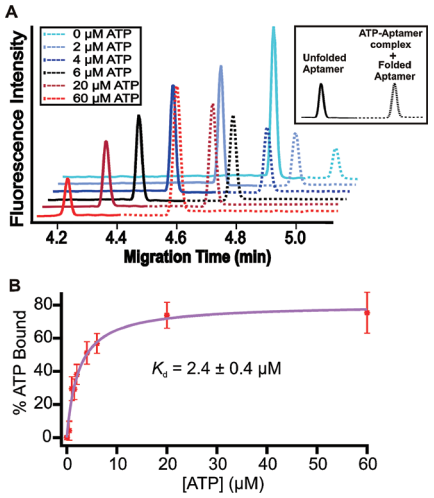

Figure 5. (A) Electropherograms for 0.5 nM aptamer in the presence of varying ATP concentrations (0–60 μM) in a 10 mM phosphate buffer (pH 7.4) containing 100 mM KCl at 25 °C. The left peak (4.2 min) represents the unfolded aptamer, while the right one (4.6 min) indicates folded aptamer species (free and ATP-bound). (B) Fraction of the ATP-bound aptamer with ATP concentration. The solid curve is a Langmuir isotherm fitting to obtain the dissociation constant, K_d.

aptamers, which is likely due to different interactions with potassium cations.[39,40] This assignment was confirmed as the folded aptamer species (the 4.6 min peak with free and ATP-bound aptamers) increase in population relative to the unfolded ones when the ATP concentration increases (Figure 5, 0–60 μM ATP traces). As a control, a scrambled sequence (see the Materials and Methods) that does not form any structures did not show this trend (see Figure S-1 in the Supporting Information). The fact that neither unfolded nor folded aptamers had tailing or fronting in the electropherogram suggests that the conversion between these two species is slow within the time scale of electrophoresis. In addition, the inseparable ATP–aptamer complex and the free folded aptamer help to maintain the equilibrium between the free and the ATP-bound aptamers during the electrophoresis. These two facts directly contrast with the nonequilibrated conditions exploited by kinetic CE for measurement of dissociation constants.[41,42]

These equilibrated conditions were used to determine the dissociation constant for the ATP–aptamer complex. First, we measured the amount of folded aptamer without bound ATP from the 4.6 min peak in the electropherogram at 0 μM ATP. By comparing the folded aptamer with the unfolded aptamer that appeared at the 4.2 min peak, we obtained a folding equilibrium constant of 0.30 (K_{fold} = [folded]/[unfolded]). This K_{fold} value is very close to that estimated from the formation probability of folded species (24%) observed in the single-molecule studies ([probability of folded]/[probability of unfolded] = 24%/76% = 0.32). With this K_{fold} value, we then determine the fraction of the free, folded aptamer in the 4.6 min peak by comparison with the unfolded aptamer population (the 4.2 min peak) for all other ATP concentrations (Figure 5, 0–60 μM ATP traces). On the basis of these fractions, a Langmuir isotherm[28] (Figure 5B) was constructed to calculate the K_d of the ATP–aptamer complex. The resultant K_d (2.4 ± 0.4 μM) matches very well with the single-molecule K_d measurement obtained above. It is also comparable with previous measurements based on affinity chromatography.[43]

dx.doi.org/10.1021/ac300427d | Anal. Chem. 2012, 84, 5298–5303

DISCUSSION

K_d Determination by Capillary Electrophoresis. Pioneered by Krylov, kinetic CE has been developed in the past 10 years to obtain the dissociation constants from nonequilibrium conditions created during capillary electrophoresis.[41] This method requires different electrophoretic mobilities between the ligand, the receptor, and the ligand−receptor complex. In addition, the binding or unbinding should be fast enough to allow the interaction to occur within the time scale of the CE separation. Here, due to the inseparable species of bound and free aptamers, and the slow folding and unfolding of the aptamer (see above), our method allows the determination of the binding affinity in a manner different from that of kinetic CE approaches. This equilibrated CE method is also different from the previous CE approaches that utilize the different mobilities between the free and bound species to obtain the binding affinity.[14] Our CE method provides a K_d value close to that from affinity chromatography (6 ± 3 μM),[43] validating our equilibrated CE approach for the affinity measurement.

K_d Determination by Laser Tweezers. Single-molecule studies can reveal detailed mechanisms of the interaction between ligands and receptors.[44] However, not many single-molecule approaches are capable of retrieving thermodynamic variables, such as K_d, which is best obtained at equilibrium established by millions of molecules. Being highly sensitive, single-molecule techniques are better suited to investigate kinetics processes. Jarzynksi's approach[45] to retrieve thermodynamic information from nonequilibrated processes greatly expands the capability of single-molecule techniques. Our methods described above fully utilize this innovative discovery. By repeatedly unfolding and refolding individual structures with a laser tweezers instrument, the change in free energy of unfolding can be obtained from nonequilibrium conditions. The single-molecule setting reduces the number of unfolding and refolding cycles that are required to retrieve the thermodynamic information as the thermal bath from the environment becomes significant at the single-molecular level. The validity of such an approach has been well established previously.[45]

The fact that the binding energy, $\Delta G_{binding}$, which is used for the dissociation constant calculation, can be obtained in the presence of a ligand with a desired concentration enables our method to determine the binding affinity from only one concentration of the ligand (Figure 3). Previously, methods have been demonstrated to measure the affinity from a ligand with a fixed concentration.[46,47] However, all these approaches require a certain range of workable concentration to ensure accurate determination of a dissociation constant. In our case, this limitation is not necessary. In practice, we can choose a ligand concentration high enough to populate ligand-bound species, from which the ΔG_{unfold} is determined (in this research, we obtained ΔG_{unfold} from the 100 μM ATP concentration). After correction for the ΔG_{unfold} for an aptamer without a bound ligand, $\Delta G_{binding}$ is obtained (Figure 4). Therefore, our method can be conveniently used to evaluate the dissociation constant without prior knowledge.

This single-molecule approach provides a general platform to measure the binding affinity of a receptor−ligand system beyond the aptamer−ligand complex described here. To investigate protein−ligand interaction, a protein can be tethered between two optically trapped particles. The mechanical stability of the protein can then be evaluated with or without a ligand to determine the dissociation constant using the Hess-like cycle (Figure 4). Recently, several proteins[48,49] have been investigated for their mechanical stabilities by laser tweezers using a similar molecular-construct strategy described here. Compared to the fluorescence-based evaluations that are prone to background noises, the force-based detection has reduced noise.[29] In addition, the positions from which a receptor is attached to handles can be well controlled to avoid the labeling impact on the binding pocket, which is common for fluorescence-based methods. Finally, the aptamer-containing single-molecule system serves as a natural platform for force-based sensing. Previously, we have described detection of single-nucleotide polymorphism (SNP) using this strategy.[29] By exploiting the versatility of aptamers, different small molecules can be detected on the basis of the increased mechanical stability of a ligand-bound aptamer.

SUMMARY

In summary, we have used two complementary methods, an ensemble-average-based CE and a single-molecule-based mechanical unfolding, to investigate the binding of ATP to an ATP aptamer. The aptamer−ligand interaction contributes to the increased mechanical stability of the complex, which leads to the determination of the dissociation constant by a Hess-like cycle. This dissociation constant is consistent with that determined by our equilibrated CE analysis and close to that measured in the literature.[50] We anticipate the methods developed here not only are useful for the determination of the binding affinity of general receptor−ligand systems in a convenient manner but also can be used to develop force-based biosensors.

ASSOCIATED CONTENT

Supporting Information

Additional information as noted in text. This material is available free of charge via the Internet at http://pubs.acs.org.

AUTHOR INFORMATION

Corresponding Author

*E-mail: E-mail:hmao@kent.edu. Phone: (330) 672-9380.

Notes

The authors declare no competing financial interest.

ACKNOWLEDGMENTS

We thank the National Science Foundation (Grant CHE-1026532) for financial support of this work.

REFERENCES

(1) Ellington, A. D.; Szostak, J. W. *Nature* **1992**, *355*, 850−852.
(2) Drabovich, A. P. B., M. V.; Musheev, M. U.; Krylov, S. N. *Anal. Chem.* **2009**, *81*, 490−494.
(3) Ikebukuro, K.; Kiyohara, C.; Sode, K. *Biosens. Bioelectron.* **2005**, *20*, 2168−2172.
(4) Javaherian, S.; Musheev, M. U.; Kanoatov, M.; Berezovski, M. V.; Krylov, S. N. *Nucleic Acids Res.* **2009**, *37*, e62.
(5) Ellington, A. D.; Szostak, J. W. *Nature* **1990**, *346*, 818−822.
(6) Tuerk, C.; Gold, L. *Science* **1990**, *249*, 505−510.
(7) Iliuk, A. B.; Hu, L.; Tao, W. A. *Anal. Chem.* **2011**, *83*, 4440−4452.
(8) Hermann, T.; Patel, D. J. *Science* **2000**, *287*, 820−825.
(9) Baker, B. R.; Lai, R. Y.; Wood, M. S.; Doctor, E. H.; Heeger, A. J.; Plaxco, K. W. *J. Am. Chem. Soc.* **2006**, *128*, 3138−3139.
(10) Bi, S.; Zhou, H.; Zhang, S. *Biosens. Bioelectron.* **2009**, *24*, 2961−2966.

(11) Stojanovic, M. N.; de Prada, P.; Landry, D. W. *J. Am. Chem. Soc.* **2000**, *122*, 11547−11548.
(12) Xia, F.; Zuo, X.; Yang, R.; Xiao, Y.; Kang, D.; Vallee-Belisle, A.; Gong, X.; Yuen, J. D.; Hsu, B. B.; Heeger, A. J.; Plaxco, K. W. *Proc. Natl. Acad. Sci. U.S.A.* **2010**, *107*, 10837−10841.
(13) Golub, E.; Pelossof, G.; Freeman, R.; Zhang, H.; Willner, I. *Anal. Chem.* **2009**, *81*, 9291−9298.
(14) Tao, L.; Kennedy, R. T. *Electrophoresis* **1997**, *18*, 112−117.
(15) Petrov, A.; Okhonin, V.; Berezovski, M.; Krylov, S. N. *J. Am. Chem. Soc.* **2005**, *127*, 17104−17110.
(16) Drabovich, A. P.; Berezovski, M. V.; Musheev, M. U.; Krylov, S. N. *Anal. Chem.* **2009**, *81*, 490−494.
(17) Connors, K. A. *Binding Constants*; John Wiley & Sons: New York, 1987.
(18) Nguyen, T.-H.; Steinbock, L. J.; Butt, H.-; Helm, M.; Berger, R. d. *J. Am. Chem. Soc.* **2011**, *133*, 2025−2027.
(19) Taylor, J. N.; Darugar, Q.; Kourentzi, K.; Willson, R. C.; Landes, C. F. *Biochem. Biophys. Res. Commun.* **2008**, *373*, 213−218.
(20) Ashkin, A.; Dziedzic, J. M.; Bjorkholm, J. E.; Chu, S. *Opt. Lett.* **1986**, *11*, 288.
(21) Greenleaf, W. J.; Frieda, K. L.; Foster, D. A.; Woodside, M. T.; Block, S. M. *Science* **2008**, *319*, 630−633.
(22) Baumann, C. G.; Smith, S. B.; Bloomfield, V. A.; Bustamante, C. *Proc. Natl. Acad. Sci. U.S.A.* **1997**, *94*, 6185−6190.
(23) Woodside, M. T.; Garcia-Garcia, C.; Block, S. M. *Curr. Opin. Chem. Biol.* **2008**, *12*, 640−646.
(24) Liphardt, J.; Onoa, B.; Smith, S. B.; Tinoco, I., Jr.; Bustamante, C. *Science* **2001**, *292*, 733−737.
(25) Neupane, K.; Yu, H.; Foster, D. A. N.; Wang, F.; Woodside, M. T. *Nucleic Acids Res.* **2011**, *39*, 7677−7687.
(26) Anthony, P. C.; Perez, C. F.; Garcia-Garcia, C.; Block, S. M. *Proc. Natl. Acad. Sci. U.S.A.* **2012**, *109*, 1485−1489.
(27) Cecconi, C.; Shank, E. A.; Bustamante, C.; Marqusee, S. *Science* **2005**, *309*, 2057−2060.
(28) Koirala, D.; Dhakal, S.; Ashbridge, B.; Sannohe, Y.; Rodriguez, R.; Sugiyama, H.; Balasubramanian, S.; Mao, H. *Nat. Chem.* **2011**, *3*, 782−787.
(29) Koirala, D.; Yu, Z.; Dhakal, S.; Mao, H. *J. Am. Chem. Soc.* **2011**, *133*, 9988−9991.
(30) Yu, Z.; Schonhoft, J. D.; Dhakal, S.; Bajracharya, R.; Hegde, R.; Basu, S.; Mao, H. *J. Am. Chem. Soc.* **2009**, *131*, 1876−1882.
(31) Luchette, P.; Abiy, N.; Mao, H. B. *Sens. Actuators, B* **2007**, *128*, 154−160.
(32) Smith, S. B.; Cui, Y. J.; Bustamante, C. *Science* **1996**, *271*, 795−799.
(33) Mao, H.; Luchette, P. *Sens. Actuators, B* **2008**, *129*, 764−771.
(34) Palassini, M.; Ritort, F. *Phys. Rev. Lett.* **2011**, *107*, 060601.
(35) Dhakal, S.; Schonhoft, J. D.; Koirala, D.; Yu, Z.; Basu, S.; Mao, H. *J. Am. Chem. Soc.* **2010**, *132*, 8991−8997.
(36) Jarzynski, C. *Phys. Rev. Lett.* **1997**, *78*, 2690−2693.
(37) German, I.; Buchanan, D. D.; Kennedy, R. T. *Anal. Chem.* **1998**, *70*, 4540−4545.
(38) Berezovski, M.; Nutiu, R.; Li, Y.; Krylov, S. N. *Anal. Chem.* **2003**, *75*, 1382−1386.
(39) Huang, C.-C.; Cao, Z.; Chang, H.-T.; Tan, W. *Anal. Chem.* **2004**, *76*, 6973−6981.
(40) Szilagyi, A.; Bonn, G. K.; Guttman, A. *J. Chromatogr., A* **2007**, *1161*, 15−21.
(41) Krylov, S. N. *Electrophoresis* **2007**, *28*, 69−88.
(42) Rundlett, K. L.; Armstrong, D. W. *Electrophoresis* **1997**, *18*, 2194−2202.
(43) Sassanfar, M.; Szostak, J. W. *Nature* **1993**, *364*, 550−553.
(44) Junker, J. P.; Ziegler, F.; Rief, M. *Science* **2009**, *323*, 633−637.
(45) Liphardt, J.; Dumont, S.; Smith, S. B.; Tinoco, I., Jr.; Bustamante, C. *Science* **2002**, *296*, 1832−1835.
(46) Berezovski, M.; Krylov, S. N. *J. Am. Chem. Soc.* **2002**, *124*, 13674−13675.
(47) Clark, S. M.; Konermann, L. *Anal. Chem.* **2004**, *76*, 7077−7083.
(48) Stigler, J.; Ziegler, F.; Gieseke, A.; Gebhardt, J. C. M.; Rief, M. *Science* **2011**, *334*, 512−516.
(49) Shank, E. A.; Cecconi, C.; Dill, J. W.; Marqusee, S.; Bustamante, C. *Nat. Chem.* **2010**, *465*, 637−640.
(50) Lin, C. H.; Patel, D. J. *Chem. Biol.* **1997**, *4*, 817−832.